

[Exploring positron characteristics utilizing two new positron-electron correlation schemes based on multiple electronic-structure calculation methods](#)

Zhang Wen-Shuai, Gu Bing-Chuan, Han Xiao-Xi, Liu Jian-Dang, Ye Bang-Jiao

Citation: Chin. Phys. B . 2015, 24(10): 107804. doi: 10.1088/1674-1056/24/10/107804

Journal homepage: <http://cpb.iphy.ac.cn>; <http://iopscience.iop.org/cpb>

What follows is a list of articles you may be interested in

[Structural, elastic, and electronic properties of sodium atoms encapsulated type-I silicon-clathrate compound under high pressure](#)

Zhang Wei, Chen Qing-Yun, Zeng Zhao-Yi, Cai Ling-Cang

Chin. Phys. B . 2015, 24(10): 107101. doi: 10.1088/1674-1056/24/10/107101

[Electronic structures and elastic properties of monolayer and bilayer transition metal dichalcogenides \$MX_2\$ \(\$M= Mo, W\$; \$X= O, S, Se, Te\$ \): A comparative first-principles study](#)

Zeng Fan, Zhang Wei-Bing, Tang Bi-Yu

Chin. Phys. B . 2015, 24(9): 097103. doi: 10.1088/1674-1056/24/9/097103

[Electronic and optical properties of lithium niobate under high pressure: A first-principles study](#)

Sang Dan-Dan, Wang Qing-Lin, Han Chong, Chen Kai, Pan Yue-Wu

Chin. Phys. B . 2015, 24(7): 077104. doi: 10.1088/1674-1056/24/7/077104

[Application of artificial neural networks to the inversion of positron lifetime spectrum](#)

An Ran, Zhang Jie, Kong Wei, Ye Bang-Jiao

Chin. Phys. B . 2012, 21(11): 117803. doi: 10.1088/1674-1056/21/11/117803

[Theoretical study on the positron annihilation in Rocksalt structured magnesium oxide](#)

Liu Jian-Dang, Zhang Jie, Zhang Li-Juan, Hao Ying-Ping, Guo Wei-Feng, Cheng Bin, Ye Bang-Jiao

Chin. Phys. B . 2011, 20(5): 057802. doi: 10.1088/1674-1056/20/5/057802

সুসংগত
— চাহিয়েসে পাই

中国物理 **B**
**Chinese
Physics B**

Volume 24 Number 11 November 2015

Formerly *Chinese Physics*

A Series Journal of the Chinese Physical Society
Distributed by IOP Publishing

Online: iopscience.iop.org/cpb
cpb.iphy.ac.cn

CHINESE PHYSICAL SOCIETY
IOP Publishing |

Chinese Physics B (First published in 1992)

Published monthly in hard copy by the Chinese Physical Society and online by IOP Publishing, Temple Circus, Temple Way, Bristol BS1 6HG, UK

Institutional subscription information: 2015 volume

For all countries, except the United States, Canada and Central and South America, the subscription rate per annual volume is UK£974 (electronic only) or UK£1063 (print + electronic).

Delivery is by air-speeded mail from the United Kingdom.

Orders to:

Journals Subscription Fulfilment, IOP Publishing, Temple Circus, Temple Way, Bristol BS1 6HG, UK
For the United States, Canada and Central and South America, the subscription rate per annual volume is US\$1925 (electronic only) or US\$2100 (print + electronic). Delivery is by transatlantic airfreight and onward mailing.

Orders to:

IOP Publishing, P. O. Box 320, Congers, NY 10920-0320, USA

© 2015 Chinese Physical Society and IOP Publishing Ltd

All rights reserved. No part of this publication may be reproduced, stored in a retrieval system, or transmitted in any form or by any means, electronic, mechanical, photocopying, recording or otherwise, without the prior written permission of the copyright owner.

Supported by the National Natural Science Foundation of China, the China Association for Science and Technology, and the Science Publication Foundation, Chinese Academy of Sciences

Editorial Office: Institute of Physics, Chinese Academy of Sciences, P. O. Box 603, Beijing 100190, China

Tel: (86-10) 82649026 or 82649519, Fax: (86-10) 82649027, E-mail: cpb@aphy.iphy.ac.cn

主管单位: 中国科学院

国际统一刊号: ISSN 1674-1056

主办单位: 中国物理学会和中国科学院物理研究所

国内统一刊号: CN 11-5639/O4

承办单位: 中国科学院物理研究所

编辑部地址: 北京 中关村 中国科学院物理研究所内

主 编: 欧阳钟灿

通 讯 地 址: 100190 北京 603 信箱

出 版: 中国物理学会

Chinese Physics B 编辑部

印刷装订: 北京科信印刷厂

电 话: (010) 82649026, 82649519

编 辑: Chinese Physics B 编辑部

传 真: (010) 82649027

国内发行: Chinese Physics B 出版发行部

“Chinese Physics B”网址:

国外发行: IOP Publishing Ltd

<http://cpb.iphy.ac.cn> (编辑部)

发行范围: 公开发行

<http://iopscience.iop.org/cpb> (IOPP)

Published by the Chinese Physical Society

顾问 Advisory Board

陈佳洱 教授, 院士
北京大学物理学院, 北京 100871

Prof. Academician Chen Jia-Er
School of Physics, Peking University, Beijing 100871, China

冯 端 教授, 院士
南京大学物理系, 南京 210093

Prof. Academician Feng Duan
Department of Physics, Nanjing University, Nanjing 210093, China

李政道 教授, 院士

Prof. Academician T. D. Lee
Department of Physics, Columbia University, New York, NY 10027, USA

李荫远 研究员, 院士
中国科学院物理研究所, 北京 100190

Prof. Academician Li Yin-Yuan
Institute of Physics, Chinese Academy of Sciences, Beijing 100190, China

丁肇中 教授, 院士

Prof. Academician Samuel C. C. Ting
LEP3, CERN, CH-1211, Geneva 23, Switzerland

杨振宁 教授, 院士

Prof. Academician C. N. Yang
Institute for Theoretical Physics, State University of New York, USA

杨福家 教授, 院士
复旦大学物理二系, 上海 200433

Prof. Academician Yang Fu-Jia
Department of Nuclear Physics, Fudan University, Shanghai 200433, China

周光召 研究员, 院士
中国科学技术协会, 北京 100863

Prof. Academician Zhou Guang-Zhao (Chou Kuang-Chao)
China Association for Science and Technology, Beijing 100863, China

王乃彦 研究员, 院士
中国原子能科学研究院, 北京 102413

Prof. Academician Wang Nai-Yan
China Institute of Atomic Energy, Beijing 102413, China

梁敬魁 研究员, 院士
中国科学院物理研究所, 北京 100190

Prof. Academician Liang Jing-Kui
Institute of Physics, Chinese Academy of Sciences, Beijing 100190, China

2012-2015

主 编 Editor-in-Chief

欧阳钟灿 研究员, 院士
中国科学院理论物理研究所,
北京 100190

Prof. Academician Ouyang Zhong-Can
Institute of Theoretical Physics, Chinese Academy of Sciences,
Beijing 100190, China

副主编 Associate Editors

赵忠贤 研究员, 院士
中国科学院物理研究所, 北京 100190

Prof. Academician Zhao Zhong-Xian
Institute of Physics, Chinese Academy of Sciences, Beijing 100190, China

杨国桢 研究员, 院士
中国科学院物理研究所, 北京 100190

Prof. Academician Yang Guo-Zhen
Institute of Physics, Chinese Academy of Sciences, Beijing 100190, China

张 杰 研究员, 院士
上海交通大学物理与天文系,
上海 200240

Prof. Academician Zhang Jie
Department of Physics and Astronomy, Shanghai Jiao Tong University,
Shanghai 200240, China

邢定钰 教授, 院士
南京大学物理学院, 南京 210093
沈保根 研究员, 院士
中国科学院物理研究所, 北京 100190
龚旗煌 教授, 院士
北京大学物理学院, 北京 100871
沈平 教授
香港科技大学物理系, 香港九龍

编辑委员 Editorial Board

2011–2016

Prof. F. R. de Boer

Prof. H. F. Braun

陈东敏 教授

冯世平 教授
北京师范大学物理系, 北京 100875

高鸿钧 研究员, 院士
中国科学院物理研究所, 北京 100190

顾长志 研究员
中国科学院物理研究所, 北京 100190

胡岗 教授
北京师范大学物理系, 北京 100875

侯建国 教授, 院士
中国科学技术大学中国科学院结构分析
重点实验室, 合肥 230026

李方华 研究员, 院士
中国科学院物理研究所, 北京 100190

闵乃本 教授, 院士
南京大学物理系, 南京 210093

聂玉昕 研究员
中国科学院物理研究所, 北京 100190

潘建伟 教授, 院士
中国科学技术大学近代物理系,
合肥 230026

沈志勋 教授

苏肇冰 研究员, 院士
中国科学院理论物理研究所,
北京 100190

孙昌璞 研究员, 院士
中国科学院理论物理研究所,
北京 100190

王思哥 研究员, 院士
北京大学物理学院, 北京 100871

夏建白 研究员, 院士
中国科学院半导体研究所,
北京 100083

洗鼎昌 研究员, 院士
中国科学院高能物理研究所,
北京 100049

向涛 研究员, 院士
中国科学院理论物理研究所,
北京 100190

谢心澄 教授
北京大学物理学院, 北京 100871

詹文龙 研究员, 院士
中国科学院, 北京 100864

朱邦芬 教授, 院士
清华大学物理系, 北京 100084

2013–2018

Prof. Antonio H. Castro Neto

Prof. Chia-Ling Chien

Prof. David Andelman

Prof. Masao Doi

Prof. Michiyoshi Tanaka

Prof. Werner A. Hofer

丁军 教授

贺贤土 研究员, 院士
北京应用物理与计算数学研究所,
北京 100088

金晓峰 教授
复旦大学物理系, 上海 200433

Prof. Academician Xing Ding-Yu
School of Physics, Nanjing University, Nanjing 210093, China

Prof. Academician Shen Bao-Gen
Institute of Physics, Chinese Academy of Sciences, Beijing 100190, China

Prof. Academician Gong Qi-Huang
School of Physics, Peking University, Beijing 100871, China

Prof. Sheng Ping
Department of Physics, The Hong Kong University of Science and Technology,
Kowloon, Hong Kong, China

van der Waals-Zeeman Institute der Universiteit van Amsterdam
Valckenierstraat 65, 1018 XE Amsterdam, **The Netherlands**
Physikalisches Institut, Universität Bayreuth, D-95440 Bayreuth, **Germany**

Prof. Dong-Min
Rowland Institute for Science, Harvard University, **USA**

Prof. Feng Shi-Ping
Department of Physics, Beijing Normal University, Beijing 100875, China

Prof. Academician Gao Hong-Jun
Institute of Physics, Chinese Academy of Sciences, Beijing 100190, China

Prof. Gu Chang-Zhi
Institute of Physics, Chinese Academy of Sciences, Beijing 100190, China

Prof. Hu Gang
Department of Physics, Beijing Normal University, Beijing 100875, China

Prof. Academician Hou Jian-Guo
Structure Research Laboratory, University of Science and Technology of
China, Hefei 230026, China

Prof. Academician Li Fang-Hua
Institute of Physics, Chinese Academy of Sciences, Beijing 100190, China

Prof. Academician Min Nai-Ben
Department of Physics, Nanjing University, Nanjing 210093, China

Prof. Nie Yu-Xin
Institute of Physics, Chinese Academy of Sciences, Beijing 100190, China

Prof. Academician Pan Jian-Wei
Department of Modern Physics, University of Science and Technology of
China, Hefei 230026, China

Prof. Shen Zhi-Xun
Stanford University, Stanford, CA 94305-4045, **USA**

Prof. Academician Su Zhao-Bing
Institute of Theoretical Physics, Chinese Academy of Sciences,
Beijing 100190, China

Prof. Academician Sun Chang-Pu
Institute of Theoretical Physics, Chinese Academy of Sciences, Beijing
100190, China

Prof. Academician Wang En-Ge
School of Physics, Peking University, Beijing 100871, China

Prof. Academician Xia Jian-Bai
Institute of Semiconductors, Chinese Academy of Sciences,
Beijing 100083, China

Prof. Academician Xian Ding-Chang
Institute of High Energy Physics, Chinese Academy of Sciences,
Beijing 100049, China

Prof. Academician Xiang Tao
Institute of Theoretical Physics, Chinese Academy of Sciences,
Beijing 100190, China

Prof. Xie Xin-Cheng
School of Physics, Peking University, Beijing 100871, China

Prof. Academician Zhan Wen-Long
Chinese Academy of Sciences, Beijing 100864, China

Prof. Academician Zhu Bang-Fen
Department of Physics, Tsinghua University, Beijing 100084, China

Physics Department, Faculty of Science, National University of Singapore,
Singapore 117546, **Singapore**

Department of Physics and Astronomy, The Johns Hopkins University,
Baltimore, MD 21218, **USA**

School of Physics and Astronomy, Tel Aviv University, Tel Aviv 69978, **Israel**

Toyota Physical and Chemical Research Institute, Yokomichi, Nagakute,
Aichi 480-1192, **Japan**

Research Institute for Scientific Measurements, Tohoku University, Katahira
2-1-1, Aoba-ku 980, Sendai, **Japan**

Stephenson Institute for Renewable Energy, The University of Liverpool,
Liverpool L69 3BX, **UK**

Prof. Ding Jun
Department of Materials Science & Engineering, National University of
Singapore, Singapore 117576, **Singapore**

Prof. Academician He Xian-Tu
Institute of Applied Physics and Computational Mathematics, Beijing 100088,
China

Prof. Jin Xiao-Feng
Department of Physics, Fudan University, Shanghai 200433, China

李儒新 研究员
中国科学院上海光学精密机械研究所,
上海 201800
吕力 研究员
中国科学院物理研究所, 北京 100190
李晓光 教授
中国科学技术大学物理系, 合肥 230026
沈元壤 教授
王亚愚 教授
清华大学物理系, 北京 100084
王玉鹏 研究员
中国科学院物理研究所, 北京 100190
王肇中 教授
闻海虎 教授
南京大学物理学院系, 南京 210093
徐至展 研究员, 院士
中国科学院上海光学精密机械研究所,
上海 201800
许岑珂 助理教授
薛其坤 教授, 院士
清华大学物理系, 北京 100084
叶军 教授

张振宇 教授

2015–2020

Prof. J. Y. Rhee
Prof. Robert J. Joynt
程建春 教授
南京大学物理学院, 南京 210093
戴希 研究员
中国科学院物理研究所, 北京 100190
郭光灿 教授, 院士
中国科学技术大学物理学院, 合
肥 230026
刘朝星 助理教授
刘荧 教授
上海交通大学物理与天文系, 上
海 200240
龙桂鲁 教授
清华大学物理系, 北京 100084
牛谦 教授
欧阳颀 教授, 院士
北京大学物理学院, 北京 100871
孙秀冬 教授
哈尔滨工业大学物理系, 哈尔滨 150001
童利民 教授
浙江大学光电信息工程学系, 杭
州 310027
童彭尔 教授
香港科技大学物理系, 香港九龍
王开友 研究员
中国科学院半导体研究所, 北京 100083
魏苏淮 教授
解思深 研究员, 院士
中国科学院物理研究所, 北京 100190
叶朝辉 研究员, 院士
中国科学院武汉物理与数学研究所,
武汉 430071
郁明阳 教授
张富春 教授
香港大学物理系, 香港
张勇 教授
郑波 教授
浙江大学物理系, 杭州 310027
周兴江 研究员
中国科学院物理研究所, 北京 100190

编辑 Editorial Staff

王久丽 Wang Jiu-Li 章志英 Zhang Zhi-Ying 蔡建伟 Cai Jian-Wei 翟振 Zhai Zhen 郭红丽 Guo Hong-Li

Prof. Li Ru-Xin
Shanghai Institute of Optics and Fine Mechanics, Chinese Academy of
Sciences, Shanghai 201800, China
Prof. Lü Li
Institute of Physics, Chinese Academy of Sciences, Beijing 100190, China
Prof. Li Xiao-Guang
Department of Physics, University of Science and Technology of China,
Hefei 230026, China
Prof. Shen Yuan-Rang
Lawrence Berkeley National Laboratory, Berkeley, CA 94720, **USA**
Prof. Wang Ya-Yu
Department of Physics, Tsinghua University, Beijing 100084, China
Prof. Wang Yu-Peng
Institute of Physics, Chinese Academy of Sciences, Beijing 100190, China
Prof. Wang Zhao-Zhong
Laboratory for Photonics and Nanostructures(LPN) CNRS-UPR20,
Route de Nozay, 91460 Marcoussis, **France**
Prof. Wen Hai-Hu
School of Physics, Nanjing University, Nanjing 210093, China
Prof. Academician Xu Zhi-Zhan
Shanghai Institute of Optics and Fine Mechanics, Chinese Academy of
Sciences, Shanghai 201800, China
Assist. Prof. Xu Cen-Ke
Department of Physics, University of California, Santa Barbara, CA 93106,
USA
Prof. Academician Xue Qi-Kun
Department of Physics, Tsinghua University, Beijing 100084, China
Prof. Ye Jun
Department of Physics, University of Colorado, Boulder,
Colorado 80309-0440, **USA**
Prof. Z. Y. Zhang
Oak Ridge National Laboratory, Oak Ridge, TN 37831–6032, **USA**

Department of Physics, Sungkyunkwan University, Suwon, **Korea**
Physics Department, University of Wisconsin-Madison, Madison, **USA**
Prof. Cheng Jian-Chun
School of Physics, Nanjing University, Nanjing 210093, China
Prof. Dai Xi
Institute of Physics, Chinese Academy of Sciences, Beijing 100190, China
Prof. Academician Guo Guang-Can
School of Physical Sciences, University of Science and Technology of China,
Hefei 230026, China
Assist. Prof. Liu Chao-Xing
Department of Physics, Pennsylvania State University PA 16802-6300, **USA**
Prof. Liu Ying
Department of Physics and Astronomy, Shanghai Jiao Tong University,
Shanghai 200240, China
Prof. Long Gui-Lu
Department of Physics, Tsinghua University, Beijing 100084 China
Prof. Niu Qian
Department of Physics, University of Texas, Austin, TX 78712, **USA**
Prof. Academician Ouyang Qi
School of Physics, Peking University, Beijing 100871, China
Prof. Sun Xiu-Dong
Department of Physics, Harbin Institute of Technology, Harbin 150001, China
Prof. Tong Li-Min
Department of Optical Engineering, Zhejiang University,
Hangzhou 310027, China
Prof. Tong Peng-Er
Department of Physics, The Hong Kong University of Science and Technology,
Kowloon, Hong Kong, China
Prof. Wang Kai-You
Institute of Semiconductors, Chinese Academy of Sciences, Beijing 100083,
China
Prof. Wei Su-Huai
National Renewable Energy Laboratory, Golden, Colorado 80401-3393, **USA**
Prof. Academician Xie Si-Shen
Institute of Physics, Chinese Academy of Sciences, Beijing 100190, China
Prof. Academician Ye Chao-Hui
Wuhan Institute of Physics and Mathematics, Chinese Academy of Sciences,
Wuhan 430071, China
Prof. Yu Ming-Yang
Theoretical Physics I, Ruhr University, D-44780 Bochum, **Germany**
Prof. Zhang Fu-Chun
Department of Physics, The University of Hong Kong, Hong Kong, China
Prof. Zhang Yong
Electrical and Computer Engineering Department, The University of North
Carolina at Charlotte, Charlotte, **USA**
Prof. Zheng Bo
Physics Department, Zhejiang University, Hangzhou 310027, China
Prof. Zhou Xing-Jiang
Institute of Physics, Chinese Academy of Sciences, Beijing 100190, China

Exploring positron characteristics utilizing two new positron–electron correlation schemes based on multiple electronic structure calculation methods*

Zhang Wen-Shuai(张文帅)^{a)b)}, Gu Bing-Chuan(谷冰川)^{a)b)}, Han Xiao-Xi(韩小溪)^{a)b)},
Liu Jian-Dang(刘建党)^{a)b)}, and Ye Bang-Jiao(叶邦角)^{a)b)†}

^{a)}Department of Modern Physics, University of Science and Technology of China, Hefei 230026, China

^{b)}State Key Laboratory of Particle Detection and Electronics, University of Science and Technology of China, Hefei 230026, China

(Received 23 April 2015; revised manuscript received 2 June 2015; published online 20 August 2015)

We make a gradient correction to a new local density approximation form of positron–electron correlation. The positron lifetimes and affinities are then probed by using these two approximation forms based on three electronic-structure calculation methods, including the full-potential linearized augmented plane wave (FLAPW) plus local orbitals approach, the atomic superposition (ATSUP) approach, and the projector augmented wave (PAW) approach. The differences between calculated lifetimes using the FLAPW and ATSUP methods are clearly interpreted in the view of positron and electron transfers. We further find that a well-implemented PAW method can give near-perfect agreement on both the positron lifetimes and affinities with the FLAPW method, and the competitiveness of the ATSUP method against the FLAPW/PAW method is reduced within the best calculations. By comparing with the experimental data, the new introduced gradient corrected correlation form is proved to be competitive for positron lifetime and affinity calculations.

Keywords: positron annihilation, positron lifetime, electronic structure

PACS: 78.70.Bj, 71.60.+z, 71.15.Mb

DOI: 10.1088/1674-1056/24/10/107804

1. Introduction

In recent decades, the Positron Annihilation Spectroscopy (PAS) has become a valuable method to study the microscopic structure of solids^[1–3] and gives detailed information on the electron density and/or momentum distribution^[4] in the regions scanned by positrons. An associated theory is required for a thorough understanding of the experimental results. A full two-component self-consistent scheme^[5,6] has been developed to calculate positron states in solids based on the density functional theory (DFT).^[7] In particular, in bulk material where the positron is delocalized and does not affect the electron states, the full two-component scheme can be reduced without losing accuracy to the conventional scheme^[5,6] in which the electronic structure is determined by common one-component formalism. However, there are various kinds of approximations that can be adjusted within this calculation. To improve the analyses of experimental data, one should find out which approximations are more credible to produce the positron state.^[8–10] In this paper, we focus on probing the positron lifetimes and affinities by using two new positron–electron correlation schemes that are based on three electronic-structure calculation methods.

Recently, Drummond *et al.*^[11,12] made two calculations for a positron immersed in a homogeneous electron gas by using the Quantum Monte Carlo (QMC) method and a modified one-component DFT method, and then two forms of local

density approximations (LDA) on the positron–electron correlation are derived. Kuriplach and Barbiellini^[8,9] proposed a fitted LDA form and a generalized gradient approximation (GGA) form based on previous QMC calculation, and then applied these two forms to multiple calculations for positron characteristics in a solid. However, the LDA form based on the modified one-component DFT calculation has not been studied. In this work, we make a gradient correction to the IDFTLDA form and validate these two new positron–electron correlation schemes by applying them to multiple positron lifetimes and affinities calculations.

We probe in detail the effect of different electronic-structure calculation methods on positron characteristics in a solid. These methods include the full-potential linearized augmented plane-wave (FLAPW) plus local orbitals method,^[13] the projector augmented wave (PAW) method,^[14] and the atomic superposition (ATSUP) method.^[15] Among these methods, the FLAPW method is regarded as the most accurate method to calculate electronic structure, the ATSUP method performs with the best computational efficiency, the PAW method has greater computational efficiency and close accuracy because the FLAPW method but has not been completely tested on positron lifetimes and affinities calculations, except for some individual calculations.^[16–19] Moreover, our previous work^[20] showed that the calculated lifetimes utilizing the PAW method disagree with those uti-

*Project supported by the National Natural Science Foundation of China (Grant Nos. 11175171 and 11105139).

†Corresponding author. E-mail: bjye@ustc.edu.cn

lizing the FLAPW method. However, within these PAW calculations, the ionic potential was not well constructed. In this paper, we investigated the influences of the ionic pseudo-potential/full-potential and different electron–electron exchange–correlations approaches within the PAW calculations. In particular, the difference between calculated lifetimes by using the self-consistent (FLAPW) and non-self-consistent (ATSUP) methods is clearly investigated in the view of positron and electron transfers.

This paper is organized as follows. In Section 2, we give a brief and overall description of the models considered here, as well as the computational details and the analysis methods we used. In Section 3, we introduce the experimental data on positron lifetime used in this work. In Section 4, we firstly apply all approximation methods for electronic-structure and positron-state calculations to the cases of Si and Al, and give detailed analyses on the effects of these different approaches, and then assess the two new correlation schemes by using the positron lifetime/affinity data in comparison with other schemes based on different electronic-structure calculation methods.

2. Theory and methodology

2.1. Theory

In this section, we briefly introduce the calculation scheme for the positron state and various approximations investigated in this work. Firstly, we do the electronic-structure calculation without considering the perturbation by positron to obtain the ground-state electronic density $n_{e-}(\mathbf{r})$ and the Coulomb potential $V_{\text{Coul}}(\mathbf{r})$ sensed by the positron. Then, the positron density is determined by solving the Kohn–Sham equation

$$\left[-\frac{1}{2}\nabla_{\mathbf{r}} + V_{\text{Coul}}(\mathbf{r}) + V_{\text{corr}}(\mathbf{r}) \right] \psi^+ = \varepsilon^+ \psi^+, \quad n_{e+}(\mathbf{r}) = |\psi^+(\mathbf{r})|^2, \quad (1)$$

where $V_{\text{corr}}(\mathbf{r})$ is the correlation potential between electron and positron. Finally, the positron lifetime can be obtained by the inverse of the annihilation rate, which is proportional to the product of positron density and electron density accompanied by the so-called enhancement factor arising from the correlation energy between a positron and electrons.^[21] The equations are written as follows:

$$\tau_{e+} = \frac{1}{\lambda}, \quad \lambda = \pi r_0^2 c \int d\mathbf{r} n_{e-}(\mathbf{r}) n_{e+}(\mathbf{r}) \gamma(n_{e-}), \quad (2)$$

where r_0 is the classical electron radius, c is the speed of light, and $\gamma(n_{e-})$ is the enhancement factor of the electron density at the position \mathbf{r} . The positron affinity can be calculated by adding electron and positron chemical potentials together:

$$A^+ = \mu^- + \mu^+. \quad (3)$$

The positron chemical potential μ^+ is determined by the positron ground-state energy. The electron chemical potential μ^- is derived from the Fermi energy (top energy of the valence band) in the case of a metal (a semiconductor). This scheme is still accurate for a perfect lattice, as in this case the positron density is delocalized and vanishingly small at every point and thus does not affect the bulk electronic structure.^[6,21]

In our calculations, each enhancement factor is applied identically to all electrons, as suggested by Jensen.^[22] These enhancement factors can be divided into two categories: the local density approximation (LDA) and the generalized gradient approximation (GGA), and they are parameterized by the following equation

$$\gamma = 1 + (1.23r_s + a_2r_s^2 + a_3r_s^3 + a_{3/2}r_s^{3/2} + a_{7/3}r_s^{7/3} + a_{8/3}r_s^{8/3}) e^{-\alpha\varepsilon}, \quad (4)$$

here, r_s is defined by $r_s = (3/4\pi n_{e-})^{1/3}$, ε is defined by $\varepsilon = |\nabla \ln(n_{e-})|^2 / q_{\text{TF}}^2$ (q_{TF}^{-1} is the local Thomas–Fermi screening length), a_2 , a_3 , $a_{3/2}$, $a_{5/2}$, $a_{7/3}$, $a_{8/3}$, and α are fitted parameters. We have investigated the five forms of the enhancement factor and the correlation potential marked by IDFTLDA,^[12] fQMCLDA,^[8,9] fQMCGGA,^[8,9] PHCLDA,^[23] and PHCGGA,^[24] plus a new GGA form IDFTGGA introduced in this work based on the IDFTLDA scheme. The fitted parameters of these enhancement factors are listed in Table 1. The LDA forms of V_{corr} corresponding to IDFTLDA, fQMCLDA, PHCLDA are given in Refs. [8], [12], and [25], respectively. Within the GGA, the corresponding correlation potential takes the form $V_{\text{corr}}^{\text{GGA}} = V_{\text{corr}}^{\text{LDA}} e^{-\alpha\varepsilon/3}$.^[26,27] The electronic density and Coulomb potential were calculated by using various methods including: a) the all-electron full potential linearized augmented plane wave plus local orbitals (FLAPW) method,^[13] as implemented in Ref. [8] which is regarded as the most accurate method to calculate electronic-structure; b) the projector augmented wave (PAW) method^[14] with reconstruction of all-electron and full-potential performing with greater computational efficiency and closer accuracy than the FLAPW method; and, c) the non-self-consistent atomic superposition (ATSUP) method,^[15] which has the best computational efficiency.

Table 1. Parameterized LDA/GGA correlation schemes.

γ	a_2	a_3	$a_{3/2}$	$a_{7/3}$	$a_{8/3}$	α
IDFTLDA	4.1698	0.1737	-1.567	-3.579	0.8364	0
IDFTGGA	4.1698	0.1737	-1.567	-3.579	0.8364	0.143
fQMCLDA	-0.22	1/6	0	0	0	0
fQMCGGA	-0.22	1/6	0	0	0	0.05
PHCLDA	-0.137	1/6	0	0	0	0
PHCGGA	-0.137	1/6	0	0	0	0.10

2.2. Computational details

In our calculations for the electronic structure we implemented the three methods that are mentioned above. For the FLAPW calculations, the WIEN2k code^[28] was used, the PBE–GGA approach^[29] was adopted for electron–electron exchange–correlations, the total number of k -points in the whole Brillouin zone (BZ) was set to 3375, and the self-consistency was achieved up to both levels of 0.0001 Ry for total energy and 0.001 e for charge distance. For the PAW calculations, the PWSCF code within the Quantum ESPRESSO package^[30] was used, the PBEsol–GGA,^[31] and PZ–LDA^[32] approaches were also implemented for electron–electron exchange–correlations besides the PBE–GGA approach, the PAW pseudo-potential files named *PSLibrary* 0.3.1 and generated by Corso (SISSA, Italy) were employed,^[33] the k -points grid was automatically generated with the parameter being set at least (333) in Monkhorst–Pack scheme, the kinetic energy cut-off of more than 100 Ry (400 Ry) for the wave-functions (charge density) and the default convergence threshold of 10^{-6} were adopted for self-consistency. For AT-SUP calculations, the electron density and Coulomb potential for each material were simply approximated by the superposition of the electron density and Coulomb potential of neutral free atoms,^[15] while the total number of the node points was set to the same as in PAW calculations. Besides, $2 \times 2 \times 2$ supercells were used to calculate the electron structures of mono-vacancy in Al and Si. To obtain the positron state, the three-dimensional Kohn–Sham equation, i.e. Eq. (1), was solved by the finite-difference method while the unit cell of each material was divided into about 10 mesh spaces per Bohr in each dimension. All of the important variable parameters were checked carefully to achieve that the computational precision of lifetime and affinities are in the order of 0.1 ps and 0.01 eV, respectively.

2.3. Model comparison

An appropriate criterion must be chosen to make a comparison between different models. The root-mean-squared deviation (RMSD) is the most popular and it is defined as the square root of the mean of the squared deviation between experimental and theoretical results: $\text{RMSD} = [\sum_{i=1}^N (X_i^{\text{exp}} - X_i^{\text{theo}})^2 / N]^{1/2}$, here N denotes the number of experimental values. In addition, since the theoretical values can be treated to be noise-free, the simple mean-absolute-deviation (MAD) defined by $\text{MAD} = \sum_{i=1}^N [|X_i^{\text{model A}} - X_i^{\text{model B}}| / N]$ is much more meaningful to quantify the overall differences between calculated results by using various models. It is obvious that the experimental data favor models producing lower values of the RMSD.

3. Experimental data

Up to five recent observed values from different literatures and groups for 21 materials were gathered to compose a reliable experimental data set. All of the experimental values for each material investigated in this work are basically collected by using the standard suggested in Ref. [57] and are listed in Table 2 with their standard deviation. Furthermore, the materials with less than five experimental measurements and/or the older experimental data were not adopted. It is reasonable to suppose that these materials have insufficient and/or unreliable experimental data that would disrupt the comparison between the models. Especially, the measurements for alkali-metals reported before 1975 are not suggested to be treated seriously.^[8] The deviations of experimental results between different groups are usually much larger than the statistical errors, even when only the recent and reliable measurements are considered. That is, the systematic error is the dominant factor, so that the sole statistical error is far from enough and is not used in this work. However, the systematic error is difficult to derive from a single experimental result. In this paper, the average experimental values of each material were used to assess the positron–electron correlation models, and the systematic errors are expected to be canceled as in Ref. [57]. Because the

Table 2. The experimental values of lifetime τ_{exp} , the related mean value τ_{exp}^* and the corresponding standard deviation σ_{exp} for each material involved in this work.

Material	τ_{exp}	τ_{exp}^*	σ_{exp}
Si	216.7 ^a 218 ^a 218 ^a 222 ^a 216 ^a	218.1	2.323
Ge	220.5 ^a 230 ^a 230 ^a 228 ^a 228 ^a	227.3	3.931
Mg	225 ^b 225 ^a 220 ^a 238 ^a 235 ^a	228.6	7.569
Al	160.7 ^a 166 ^a 163 ^a 165 ^a 165 ^a	163.9	2.114
Ti	147 ^b 154 ^a 145 ^a 152 ^a 143 ^a	148.2	4.658
Fe	108 ^a 106 ^a 114 ^a 110 ^a 111 ^a	109.8	3.033
Ni	109.8 ^a 107 ^a 105 ^a 109 ^a 110 ^a	108.2	2.127
Zn	148 ^b 153 ^a 145 ^a 154 ^a 152 ^a	150.4	3.781
Cu	110.7 ^a 122 ^a 112 ^a 110 ^a 120 ^a	114.9	2.514
Nb	119 ^a 120 ^a 122 ^a 122 ^a 125 ^a	121.6	2.302
Mo	109.5 ^a 103 ^a 118 ^a 114 ^a 104 ^a	109.7	6.418
Ta	116 ^b 122 ^a 120 ^a 125 ^a 117 ^a	120.0	3.674
Ag	120 ^a 130 ^a 131 ^a 133 ^c 131 ^b	129.0	5.147
Au	117 ^a 113 ^a 113 ^a 117 ^a 123 ^a	116.6	4.098
Cd	175 ^b 184 ^a 167 ^a 172 ^a 186 ^a	176.8	8.043
In	194.7 ^a 200 ^a 192 ^a 193 ^a 189 ^a	193.7	4.066
Pb	194 ^b 200 ^a 204 ^a 200 ^a 209 ^a	201.4	5.550
GaAs	231.6 ^d 231 ^e 230 ^f 232 ^e 220 ^h	228.9	5.043
InP	241 ⁱ 240 ^j 247 ^k 242 ^l 244 ^m	242.8	2.775
ZnO	153 ⁿ 159 ^o 158 ^p 161 ^q 171 ^r	160.4	6.618
CdTe	284 ^s 285 ^t 285 ^u 289 ^v 291 ^w	286.8	3.033

^aRef. [34], ^bRef. [35], ^cRef. [36], ^dRef. [37], ^eRef. [38], ^fRef. [39], ^hRef. [40], ^hRef. [41], ⁱRef. [42], ^jRef. [43], ^kRef. [44], ^lRef. [45], ^mRef. [46], ⁿRef. [47], ^oRef. [48], ^pRef. [49], ^qRef. [50], ^rRef. [51], ^sRef. [52], ^tRef. [53], ^uRef. [54], ^vRef. [55], ^wRef. [56]

observed values for defect state are insufficient and/or largely scattered, it is hard to make a clear discussion on the defect state by using these positron–electron correlation models in this paper. Thus, except for the detailed analyses in the cases of Si and Al based on three usually applied approaches for electronic-structure calculations, we mainly focus on testing the correlation models by using bulk materials' lifetime data and positron-affinity data. The experimental data of positron affinity are listed in Table 5.

4. Results and discussion

4.1. Detailed analyses in cases of Si and Al

Representatively, panels (a) and (c) in Fig. 1 (Fig. 2) show, respectively, the self-consistent all-electron and positron densities on plane (110) for Al (Si) based on the FLAPW method together with the fQMC-GGA form of the enhancement factor and correlation potential. It is reasonable to obtain that the panel (a) in Fig. 2 shows clear bonding states of Si while the panel (a) in Fig. 1 shows the presence of the nearly free conduction electrons in interstitial regions. To make a comparison between the FLAPW and ATSUP methods for electronic-structure calculations, we also plot the ratio of their respective all-electron and positron densities in panels (b) and (d) in Fig. (Fig.) for Al (Si). These four ratio panels actually reflect the electron and positron transfers from densities based on the non-self-consistent free atomic calculations to that based on the exact self-consistent calculations. This confirms the fact that the positron density follows the changes of the electron density, which yield a small difference in the annihilation rate between these two calculations.^[15]

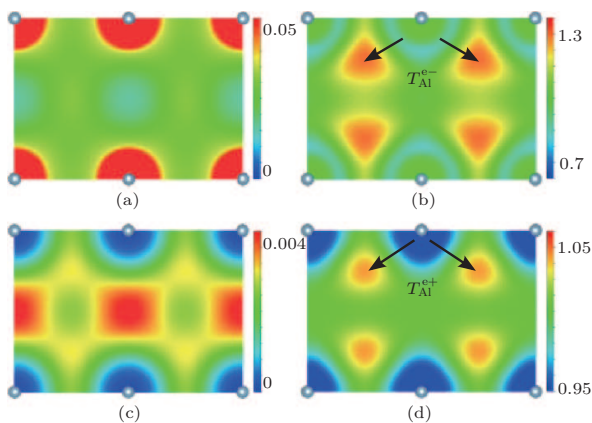


Fig. 1. (color online) The self-consistent all-electron density ρ_{FLAPW}^{e-} (a) and positron density $\rho_{\text{FLAPW}}^{e+}/\rho_{\text{ATSUP}}^{e-}$ (c) (in unit of a.u., a.u. expresses atomic unit) on plane (110) for Al based on the FLAPW method and the fQMC-GGA approximation. The ratios of all-electron density $\rho_{\text{FLAPW}}^{e-}/\rho_{\text{ATSUP}}^{e-}$ (b) or positron density $\rho_{\text{FLAPW}}^{e+}/\rho_{\text{ATSUP}}^{e+}$ (d) calculated by using the FLAPW method to that by using the ATSUP method.

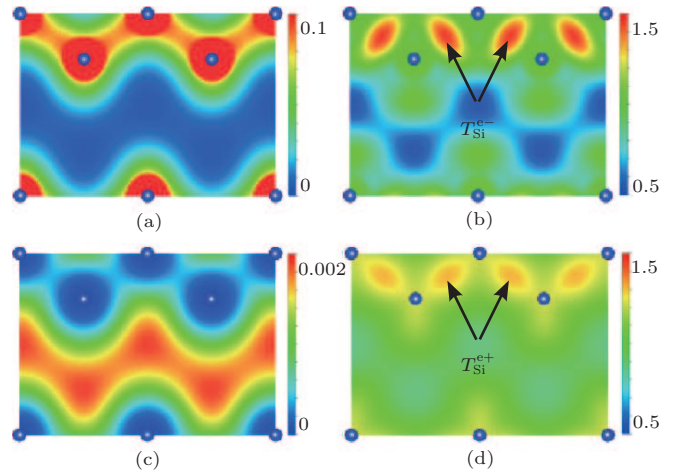


Fig. 2. (color online) The same as Fig. 1, but for Si.

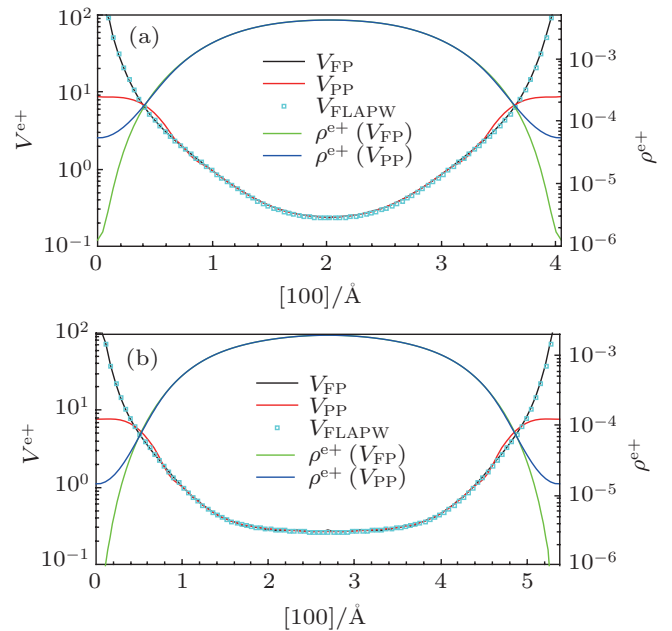


Fig. 3. (color online) The total Coulomb potential V^{e+} (in unit of Ry) sensed by the positron based on the ionic pseudo-potentials (V_{PP}) and reconstructed ionic full-potential (V_{FP}) and the corresponding calculated positron densities ρ^{e+} (in unit of a.u.) along the [100] direction between two adjacent atoms for Al (a) and Si (b), respectively. To make a further comparison, the full-potentials calculated by using the FLAPW method (V_{FLAPW}) are also plotted.

Now, taking more subtle analyses, the change of lifetime within the FLAPW calculation from that within the ATSUP calculation for Al is attributed to the competition between the following two factors: (i) the lifetime is decreased by the translations of electrons (illustrated in Fig. 1(b) as T_{Al}^{e-}) from near-nucleus regions with tiny positron densities to interstitial regions with large positron densities; and, (ii) the lifetime is increased by the translation of positron (illustrated in Fig. 1(d) as T_{Al}^{e+}) from core regions with large electron densities to interstitial regions with small electron densities. However, in the case of Si with bonding states, the change of lifetime depends conversely on the translations of electrons and positron:

a) the lifetime is increased by the translations of electrons (illustrated in Fig. 2(b) as T_{Si}^{e-}) from interstitial regions with the largest positron densities to bonding regions with tiny positron densities; and, b) the lifetime is decreased by the translation of positron (illustrated in Fig. 2(d) as T_{Si}^{e+}) from the interstitial regions with tiny electron densities to bonding regions with large electron densities. Taking note of the magnitude of scale rulers, these two figures state clearly that the translations of electrons (T^{e-}) are dominant factors for both Al and Si. Consequently, the lifetimes within the FLAPW calculations become smaller (larger) for Al (Si). These variances are proved by calculated values of lifetimes listed in Table 3. In addition, the lifetimes of Si calculated by using three GGA forms of the enhancement factor show greater differences since the large electron-density gradient terms in bonding regions giving decreases of the enhancement factor can further weaken the effect of the translation T_{Si}^{e+} .

We calculated the bulk lifetimes for Al and Si based on the PAW method. In Table 3, the label “PAW” without a suffix indicates that the electron structure is calculated by using the PBE–GGA electron–electron exchange–correlations approach^[32] and the positron-state is calculated by using reconstructed ionic full-potential (FP), the suffix “–PZ” indicates that the PBE–GGA approach is replaced by the PZ–LDA approach^[32] during electron-structure calculations, and the suffix “–PP” indicates that ionic full-potential (FP) is replaced by the ionic pseudo-potential (PP) during positron-state calculations. The ionic potential together with the Hartree potential from the valence electrons compose the total Coulomb potential in Eq. (1). It can be easily found that better implementing the PAW method by using a reconstructed full-potential can give a startling agreement with the FLAPW method on the positron-lifetime calculations for Al and Si. By comparing the results of PAW and PAW–PP approaches, the PAW–PP approach leads to smaller lifetimes with the differences up to 3.8 ps and 4.3 ps for Al and Si, respectively. These decreases are caused by the fact that the softer potential within the PAW–PP approach more powerfully attracts positron into the near-nucleus regions with much larger electron densities. This statement is illustrated by the Fig. 3 showing the total Coulomb potential V^{e+} sensed by the positron based on the ionic pseudo-potential (V_{PP}) and reconstructed ionic full-potential (V_{FP}) and the corresponding calculated positron densities ρ^{e+} along the [100] direction between two adjacent atoms for Al (a) and Si (b), respectively. To make a further comparison, the full-potentials calculated by using the FLAPW method (V_{FLAPW}) are also plotted and they are found to be nearly the same as the reconstructed PAW full-potentials. This figure indicates that a change in the ionic potential approaches (FP or PP) can lead to a change of more than one order of magnitude in the positron densities near the nuclei. It should be noted that, in the cases of PAW calculations with

underestimated core/semicore electron densities in the near-nucleus regions,^[58] the effect of overestimated positron densities based on the pseudo-potentials can be canceled, and then the excellent quality on the calculated positron lifetimes is able to be achieved. It is clear that the differences between the results of PAW–PZ and PAW are of the order of 0.1 ps, and therefore the effect of different electron–electron exchange–correlations schemes is small. We also calculated the lifetimes by using the PBEsol–GGA approach,^[31] which is revised for solids and their surfaces, and similar differences of the order of 0.1 ps are also obtained compared with the PBE–GGA approach.

Table 3. Calculated results of positron lifetimes (in unit of ps) for Al, Si, and ideal monovacancy in Al and Si based on various methods for electronic-structure and positron-state calculations.

		IDFT GGA	IDFT LDA	fQMC GGA	fQMC LDA	PHC GGA	PHC LDA
Al	ATSUP	160.778	152.470	173.347	169.357	163.036	156.438
	FLAPW	156.615	149.852	169.972	166.530	159.397	153.878
	PAW	156.649	149.898	170.016	166.584	159.432	153.925
	PAW–PP	154.113	146.814	166.507	162.798	156.574	150.587
	PAW–PZ	157.208	150.204	170.421	166.906	159.898	154.220
Si	ATSUP	201.770	186.634	213.260	207.345	201.363	190.484
	FLAPW	211.843	188.285	217.520	208.477	208.639	191.790
	PAW	211.779	188.245	217.466	208.431	208.586	191.752
	PAW–PP	208.407	184.675	213.320	204.125	205.060	187.976
	PAW–PZ	211.248	188.388	217.399	208.625	208.247	191.905
V_{Al}	ATSUP	229.441	216.639	246.294	240.941	229.686	220.274
	PAW	212.176	201.245	229.481	224.429	214.050	205.570
V_{Si}	ATSUP	227.458	208.972	239.524	232.309	225.922	212.690
	PAW	236.052	208.712	241.816	231.443	231.504	212.145

In addition, as shown in Table 3, the positron lifetimes for monovacancy in Al and Si are calculated based on the ATSUP and PAW methods for electronic-structure calculations and six correlation schemes for positron-state calculations. The ideal monovacancy structure is used in these calculations, which means that the positron is trapped into a single vacancy without considering the ionic relaxation from the ideal lattice positions. Larger differences between the results of ATSUP and PAW are found in monovacancy-state calculations compared with that in bulk-state calculations. Besides, the IDFTGGA/IDFTLDA correlation schemes produce similar lifetime values compared with the PHCGGA/PHCLDA correlation schemes and produce much smaller lifetime values compared with the fQMC GGA/fQMC LDA correlation schemes in both monovacancy-state and bulk-state calculations.

4.2. Positron lifetime calculations

In this subsection we firstly give visualized comparisons between experimental values and calculated results based on different methods for electronic-structure and positron-state calculations. Within the PAW, the positron lifetimes are all

calculated by using the reconstructed full-potential and, certainly, all-electron densities from now on.

The deviations of the theoretical results from the experimental data along with the standard deviations of observed values for all materials are plotted in Fig. 4. The scattering regions of calculated results by different forms of the enhancement factor are found to be much larger in the atom systems with bonding states compared with that in pure metal systems. Besides, the deviations of the results found by using the ATSUP method from those found by using the FLAPW method are mostly larger in GGA approximations compared with those in LDA approximations. Numerically, the MADs for different forms of the enhancement factor between the calculated lifetimes by using the ATSUP method and those by using the FLAPW method are shown in Table 4. These MADs range from 1.936 ps (PHCLDA) to 5.068 ps (IDFTGGA). Moreover, the well implemented PAW method is found to be able to give nearly the same results as the FLAPW method. Numerically, the MADs between the calculated lifetimes by the PAW method and those by the FLAPW method for different forms of the enhancement factor are also shown in Table 4. These MADs range from 0.253 ps (IDFTLDA) to 0.316 ps (IDFTGGA). This near-perfect agreement between the PAW method and the FLAPW method proves that our calculations are quite credible.

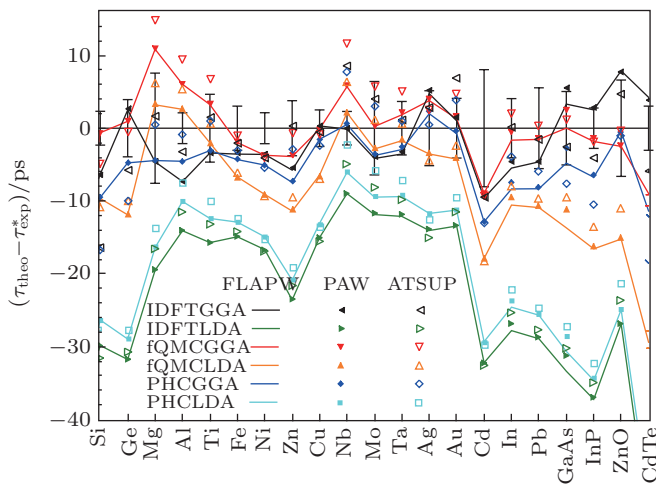


Fig. 4. (color online) The deviations of the theoretical results based on various methods from the experimental values along with the standard deviation of experimental values for each material.

Table 4. The MADs between the calculated results by using the ATSUP/PAW method and that by using the FLAPW method, and the RMSDs between the theoretical results and the experimental data τ_{exp}^* .

	MAD/ps		RMSD/ps		
	ATSUP	PAW	FLAPW	PAW	ATSUP
fQMC GGA	2.503	0.303	4.503	4.591	6.309
IDFTGGA	5.068	0.316	4.809	4.821	5.611
PHCGGA	3.667	0.287	6.148	6.013	7.672
fQMCLDA	2.184	0.290	11.36	11.19	10.35
IDFTLDA	1.966	0.253	25.19	24.99	23.88
PHCLDA	1.936	0.260	22.83	22.63	21.54

Table 4 also presents the RMSDs between the theoretical results and the experimental data τ_{exp}^* by using six positron–electron correlation schemes. Two interesting phenomena can be found in this table. Firstly, the RMSDs produced by the IDFTLDA scheme are always worse among the RMSDs based on three electron structure approaches, but are similar to those produced by the PHCLDA scheme. Thus, the gradient correction (IDFTGGA) to this LDA form (IDFTLDA) is needed. It is clear that the corrected IDFTGGA scheme largely improves the calculations and performs better than the PHCGGA scheme but is still worse than the fQMC GGA scheme. The fQMC GGA scheme together with the FLAPW method produced the best RMSD. This fact indicates that the quantum Monte Carlo calculation implemented in Ref. [11] is more credible than the modified one-component DFT calculation^[12] on the positron–electron correlation. Secondly, compared to the RMSD produced by using the FLAPW/PAW method, the RMSD produced by using the simple ATSUP method is a little smaller based on the LDA correlation schemes but is distinctly larger based on the GGA (especially fQMC GGA) correlation schemes. This phenomenon implies that the benefit of the exact electronic-structure calculation approach (PAW/FLAPW) is swamped by the inaccurate approximation of the enhancement factor. Meanwhile, the competitiveness of the ATSUP approach against the FLAPW/PAW method is reduced based on the most accurate positron–electron correlation schemes.

4.3. Positron affinity calculations

The positron affinity A^+ is an important bulk property which describes the positron energy level in a solid, and which allows us to probe the positron behavior in an inhomogeneous material. For example, the difference of the lowest positron energies between two elemental metals in contact is given by the positron affinity difference, and this determines how the positron samples behave near the interface region. Besides, if the electron work function ϕ^- is known, then the positron work function ϕ^+ can be derived by the equation: $\phi^+ = -\phi^- - A^+$. The crystal (e.g., W metal) with a stronger negative positron work function can emit a slow-positron to the vacuum from the surface and, therefore, can be utilized as a more efficient positron moderator for the slow-positron beam.

The theoretical and experimental positron affinities for eight common materials by using the new IDFTLDA and IDFTGGA correlation schemes are listed in Table 5. To make a comparison, the results corresponding to the PHCGGA and fQMC GGA schemes are also listed. During the electron structure calculation, the ATSUP method was not implemented because the ATSUP method is inappropriate for positron energetics calculations and gives much negative positron work functions.^[15] Within PAW calculations, both PBE–GGA and PZ–LDA approaches are used for electron–electron exchange correlations. The RMSDs between theoretical and experimental positron affinities are also presented in Table 5.

Table 5. Theoretical and experimental positron affinities A^+ (in unit of eV) based on four positron–electron correlation schemes and several electron structure calculation methods. The RMSDs between the theoretical and experimental positron affinities are also presented. Here, the PZ–LDA approach is labeled by PZ, and the PBE–LDA approach is labeled by PBE for short.

A^+	IDFTGGA			IDFTLDA			PHCGGA			fQMC GGA			Exp.
	FLAPW	PAW		FLAPW	PAW		FLAPW	PAW		FLAPW	PAW		
		PBE	PBE		PZ	PBE		PBE	PZ		PBE	PBE	
Si	-6.481	-6.478	-6.683	-6.884	-6.881	-7.070	-6.728	-6.726	-6.926	-6.182	-6.179	-6.373	-6.2
Al	-4.497	-4.504	-4.683	-4.624	-4.631	-4.813	-4.641	-4.648	-4.828	-3.981	-3.988	-4.169	-4.1
Fe	-3.914	-3.877	-4.290	-4.323	-4.289	-4.707	-4.120	-4.084	-4.498	-3.544	-3.508	-3.925	-3.3
Cu	-4.381	-4.437	-4.932	-4.875	-4.933	-5.435	-4.614	-4.671	-5.168	-4.073	-4.130	-4.630	-4.3
Nb	-3.847	-3.841	-4.085	-4.112	-4.107	-4.355	-4.020	-4.014	-4.260	-3.399	-3.394	-3.641	-3.8
Ag	-5.147	-5.083	-5.577	-5.670	-5.615	-6.109	-5.398	-5.337	-5.831	-4.875	-4.817	-5.310	-5.2
W	-1.956	-1.982	-2.304	-2.225	-2.254	-2.580	-2.121	-2.149	-2.472	-1.491	-1.520	-1.844	-1.9
Pb	-5.954	-5.936	-6.305	-6.328	-6.305	-6.683	-6.186	-6.166	-6.538	-5.622	-5.601	-5.977	-6.1
RMSD	0.285	0.283	0.546	0.570	0.566	0.899	0.431	0.427	0.740	0.314	0.314	0.272	–

As in previous lifetime calculations, the calculated positron affinities found by using the FLAPW method are also nearly the same as that by using the PAW method. Besides, our calculated positron affinities that are found by using the fQMC GGA & PZ–LDA approaches are in excellent agreement with those reported in Ref. [8] with a MAD being 0.06 eV. Moreover, the differences between the RMSDs produced by using the PBE–GGA and PZ–LDA approaches are not negligible and the PBE–GGA approach performs much better than the PZ–LDA approach, except for the case related to fQMC GGA. In addition, the gradient correction (IDFTGGA) to the IDFTLDA form is needed to improve the performance for positron affinity calculations. Meanwhile, the IDFTGGA correlation scheme makes distinct improvement upon positron affinity calculations compared with the PHCGGA scheme, which is similar to the cases of positron lifetime calculations of bulk materials. Nevertheless, the best agreement between the calculated and experimental positron affinities is still given by the fQMC GGA & PZ–LDA approaches.

5. Conclusion

In this work, we probe the positron lifetimes and affinities utilizing two new positron–electron correlation schemes (IDFTLDA and IDFTGGA) that are based on three common electronic-structure calculation methods (ATSUP, FLAPW, and PAW). Firstly, we apply all approximation methods for electronic-structure and positron-state calculations to the cases of Si and Al, and give detailed analyses on the effects of these different approaches. In particular, the difference between calculated lifetimes by using the self-consistent (FLAPW) and non-self-consistent (ATSUP) methods is clearly investigated in the view of positron and electron transfers. The well implemented PAW method with reconstruction of all-electron and full-potential is found to be able to give near-perfect agreement with the FLAPW method, which proves that our calculations are quite credible. Meanwhile, the competitiveness of

the ATSUP method against the FLAPW method is reduced by utilizing the best positron–electron correlation schemes (fQMC GGA). We then assess the two new positron–electron correlation schemes, the IDFTLDA form and the IDFTGGA form, by using a reliable experimental data on the positron lifetimes and affinities of bulk materials. The gradient correction (IDFTGGA) to the IDFTLDA form introduced in this work is necessary to promote the positron affinity and/or lifetime calculations. Moreover, the IDFTGGA performs better than the PHCGGA scheme in both positron affinity and lifetime calculations. However, the best agreement between the calculated and experimental positron lifetimes/affinities is obtained by using the fQMC GGA positron–electron correlation scheme. Nevertheless, the new introduced gradient corrected correlation form (IDFTGGA) is currently competitive for positron lifetime and affinity calculations.

Acknowledgment

We would like to thank Han Rong-Dian, Li Jun and Huang Shi-Juan for the helpful discussions. Part of the numerical calculations in this paper were completed on the supercomputing system in the Supercomputing Center of the University of Science and Technology of China.

References

- [1] Tuomisto F and Makkonen I 2013 *Rev. Mod. Phys.* **85** 1583
- [2] Yuan D Q, Zheng Y N, Zuo Y, *et al.* 2014 *Chin. Phys. Lett.* **31** 046101
- [3] Li Y F, Shen T L, Gao X, *et al.* 2014 *Chin. Phys. Lett.* **31** 036101
- [4] Makkonen I, Ervasti M M, Siro T and Harju A 2014 *Phys. Rev. B* **89** 041105
- [5] Nieminen R M, Boronksi E and Lantto L J 1985 *Phys. Rev. B* **32** 1377
- [6] Puska M J, Seitsonen A P and Nieminen R M 1995 *Phys. Rev. B* **52** 10947
- [7] Kohn W and Sham L J 1965 *Phys. Rev.* **140** A1133
- [8] Kuriplach J and Barbiellini B 2014 *Phys. Rev. B* **89** 155111
- [9] Kuriplach J and Barbiellini B 2014 *J. Phys.: Conf. Ser.* **505** 012040
- [10] Zhang W, Gu B, Liu J and Ye B 2015 *Comput. Mater. Sci.* **105** 32
- [11] Drummond N D, López Ríos P, Needs R J and Pickard C J 2011 *Phys. Rev. Lett.* **107** 207402

- [12] Drummond N D, López Ríos P, Pickard C J and Needs R J 2010 *Phys. Rev. B* **82** 035107
- [13] Sjöstedt E, Nordström L and Singh D J 2000 *Solid State Commun.* **114** 15
- [14] Blöchl P E 1994 *Phys. Rev. B* **50** 17953
- [15] Puska M J and Nieminen R M 1983 *J. Phys. F: Met. Phys.* **13** 333
- [16] Wiktor J, Kerbirou X, Jomard G, Esnouf S, Barthe M F and Bertolus M 2014 *Phys. Rev. B* **89** 155203
- [17] Wiktor J, Barthe M F, Jomard G, Torrent M, Freyss M and Bertolus M 2014 *Phys. Rev. B* **90** 184101
- [18] Makkonen I, Hakala M and Puska M J 2006 *Phys. Rev. B* **73** 035103
- [19] Rauch C, Makkonen I and Tuomisto F 2011 *Phys. Rev. B* **84** 125201
- [20] Huang S J, Zhang W S, Liu J D, Zhang J, Li J and Ye B J 2014 *Acta Phys. Sin.* **63** 217804 (in Chinese)
- [21] Boroński E and Nieminen R M 1986 *Phys. Rev. B* **34** 3820
- [22] Jensen K O 1989 *J. Phys.: Condens. Matter* **1** 10595
- [23] Stachowiak H and Lach J 1993 *Phys. Rev. B* **48** 9828
- [24] Boroński E 2010 *Nukleonika* **55** 9
- [25] Boroński E and Stachowiak H 1998 *Phys. Rev. B* **57** 6215
- [26] Barbiellini B, Puska M J, Torsti T and Nieminen R M 1995 *Phys. Rev. B* **51** 7341
- [27] Barbiellini B, Puska M J, Korhonen T, Harju A, Torsti T and Nieminen R M 1996 *Phys. Rev. B* **53** 16201
- [28] Blaha P, Schwarz K, Madsen G K H, Kvasnicka D and Luitz J 2001 WIEN2k, An Augmented Plane Wave Plus Local Orbitals Program for Calculating Crystal Properties, Vienna University of Technology, Austria, 2001
- [29] Perdew J P, Burke K and Ernzerhof M 1996 *Phys. Rev. Lett.* **77** 3865
- [30] Giannozzi P, Baroni S, Bonini N, et al. 2009 *J. Phys.: Condens. Matter* **21** 395502
- [31] Perdew J P, Ruzsinszky A, Csonka G I, Vydrov O A, Scuseria G E, Constantin L A, Zhou X and Burke K 2008 *Phys. Rev. Lett.* **100** 136406
- [32] Perdew J P and Zunger A 1981 *Phys. Rev. B* **23** 5048
- [33] Corso A D 2014 *Comput. Mater. Sci.* **95** 337
- [34] Campillo Robles J M and Plazaola F 2003 *Defect Diffus. Forum* **213–215** 141
- [35] Seeger A, Barnhart F and W B 1989 in *Positron Annihilation*, eds. Dorikens-Vanpraet L, Dorikens M and Segers D (Singapore: World Scientific) p. 275s; see also Sterne P A, Kaiser J H 1991 *Phys. Rev. B* **43** 13892; and Jensen K O 1989 *J. Phys.: Condens. Matter* **1** 10595
- [36] Welch D O and Lynn K G 1976 *Phys. Status Solidi B* **77** 277
- [37] Wang Z, Wang S J, Chen Z Q, Ma L and Li S 2000 *Phys. Stat. Sol.* **177** 341
- [38] Saarinen K, Hautojärvi P, Lanki P and Corbel C 1991 *Phys. Rev. B* **44** 10585
- [39] Polity A, Rudolf F, Nagel C, Eichler S and Krause-Rehberg R 1997 *Phys. Rev. B* **55** 10467
- [40] Dlubek G, Krause R, Brümmer O and Tittes J 1987 *Appl. Phys. A: Solids Surf.* **42** 125
- [41] Dannefaer S, Hogg B and Kerr D 1984 *Phys. Rev. B* **30** 3355
- [42] Beling C D, Deng A H, Shan Y Y, Zhao Y W, Fung S, Sun N F, Sun T N and Chen X D 1998 *Phys. Rev. B* **58** 13648
- [43] Chen Z Q, Hu X W and Wang S J 1998 *Appl. Phys. A: Solids Surf.* **66** 435
- [44] Puska M J, Mäkinen S, Manninen M and Nieminen R M 1989 *Phys. Rev. B* **39** 7666
- [45] Dlubek G and Brümmer O 1986 *Ann. Phys. (Leipzig)* **7** 178
- [46] Dlubek G, Brümmer O, Plazaola F, Hautojärvi P and Naukkarinen K 1985 *Appl. Phys. Lett.* **46** 1136
- [47] Mizuno M, Araki H and Shirai Y 2004 *Mater. Trans.* **45** 1964
- [48] Brauer G, Anwand W, Skorupa W, Kuriplach J, Melikhova O, Moisson C, Wenckstern H, Schmidt H, Lorenz M and Grundmann M 2006 *Phys. Rev. B* **74** 045208
- [49] Uedono A, Koida T, Tsukazaki A, Kawasaki M, Chen Z Q, Chichibu S and Koinuma H 2003 *J. Appl. Phys.* **93** 2481
- [50] Brunner S, Puff W, Balogh A G and Mascher P 2001 *Mater. Sci. Forum* **363–365** 141
- [51] Tuomisto F, Ranki V, Saarinen K and Look D C 2003 *Phys. Rev. Lett.* **91** 205502
- [52] Plazaola F, Seitsonen A P and Puska M J 1994 *J. Phys.: Condens. Matter* **6** 8809
- [53] Gély-Sykes C, Corbel C and Triboulet R 1993 *Solid State Commun.* **80** 79
- [54] Peng Z L, Simpson P J and Maschera P 2000 *Electrochem. Solid-State Lett.* **3** 150
- [55] Geffroy B, Corbel C, Stucky M, Triboulet R, Hautojärvi P, Plazaola F L, Saarinen K, Rajainmäki H, Aaltonen J, Moser P, Sengupta A and Pautrat J L 1986 *Defects in Semiconductors*, ed. H. J. von Bardeleben, *Materials Science Forum* (Aedermannsdorf: Trans. Tech. Publications) Vol. 10–12, p. 1241
- [56] Dannefaer S 1982 *J. Phys. C* **15** 599
- [57] Campillo Robles J M, Ogando E and Plazaola F 2007 *J. Phys.: Condens. Matter* **19** 176222
- [58] Tang Z, Hasegawa M, Nagai Y, Saito M and Kawazoe Y 2002 *Phys. Rev. B* **65** 045108

JUST FOR AUTHORS
— CHINESE PHYSICS B

Chinese Physics B

Volume 24

Number 10

October 2015

GENERAL

- 100101 Rapid identifying high-influence nodes in complex networks**
Song Bo, Jiang Guo-Ping, Song Yu-Rong and Xia Ling-Ling
- 100201 Singular and non-topological soliton solutions for nonlinear fractional differential equations**
Ozkan Guner
- 100202 Analysis of elastoplasticity problems using an improved complex variable element-free Galerkin method**
Cheng Yu-Min, Liu Chao, Bai Fu-Nong and Peng Miao-Juan
- 100203 Conservative method for simulation of a high-order nonlinear Schrödinger equation with a trapped term**
Cai Jia-Xiang, Bai Chuan-Zhi and Qin Zhi-Lin
- 100204 Transformation optics for efficient calculation of transmembrane voltage induced on cells**
Liao Yin-Hong, Zhu Hua-Cheng, Tang Zheng-Ming and Huang Ka-Ma
- 100301 Time-domain nature of group delay**
Wang Jian-Wu and Feng Zheng-He
- 100302 A new kind of special function and its application**
Fan Hong-Yi, Wan Zhi-Long, Wu Ze and Zhang Peng-Fei
- 100303 Shannon information entropies for position-dependent mass Schrödinger problem with a hyperbolic well**
Sun Guo-Hua, Dušan Popov, Oscar Camacho-Nieto and Dong Shi-Hai
- 100304 Characterizing the dynamics of quantum discord under phase damping with POVM measurements**
Jiang Feng-Jian, Ye Jian-Feng, Yan Xin-Hu and Lü Hai-Jiang
- 100305 Non-Markovianity of a qubit coupled with an isotropic Lipkin–Meshkov–Glick bath**
Tian Li-Jun, Ti Min-Min and Zhai Xiang-Dong
- 100306 Scheme for purifying a general mixed entangled state and its linear optical implementation**
Dong Dong, Zhang Yan-Lei, Zou Chang-Ling, Zou Xu-Bo and Guo Guang-Can
- 100307 Deterministic joint remote state preparation of arbitrary single- and two-qubit states**
Chen Na, Quan Dong-Xiao, Xu Fu-Fang, Yang Hong and Pei Chang-Xing
- 100501 A perturbation method to the tent map based on Lyapunov exponent and its application**
Cao Lv-Chen, Luo Yu-Ling, Qiu Sen-Hui and Liu Jun-Xiu
- 100502 A novel adaptive-impulsive synchronization of fractional-order chaotic systems**
Leung Y. T. Andrew, Li Xian-Feng, Chu Yan-Dong and Zhang Hui
- 100503 Synchronization of coupled chaotic Hindmarsh Rose neurons: An adaptive approach**
Wei Wei
- 100504 Dynamics and stabilization of peak current-mode controlled buck converter with constant current load**
Leng Min-Rui, Zhou Guo-Hua, Zhang Kai-Tun and Li Zhen-Hua

(Continued on the Bookbinding Inside Back Cover)

ATOMIC AND MOLECULAR PHYSICS

- 103201 The ac Stark shifts of the terahertz clock transitions of barium**
Yu Geng-Hua, Geng Ying-Ge, Li Long, Zhou Chao, Duan Cheng-Bo, Chai Rui-Peng and Yang Yong-Ming
- 103202 Extreme ultraviolet and x-ray transition wavelengths in Rb XXIV**
Indu Khatri, Arun Goyal, Sunny Aggarwal, A. K. Singh and Man Mohan
- 103203 Role of elastic scattering in high-order above threshold ionization**
Chen Zhang-Jin, Ye Jian-Mian and Xu Yang-Bing
- 103204 The VMI study on angular distribution of ejected electrons from Eu $4f^7 6p_{1/2} 6d$ autoionizing states**
Zhang Kai, Shen Li, Dong Cheng and Dai Chang-Jian
- 103401 Resonant charge transfer in slow $\text{Li}^+ - \text{Li}(2s)$ collisions**
Li Tie-Cheng, Liu Chun-Hua, Qu Yi-Zhi, Liu Ling, Wu Yong, Wang Jian-Guo, Liebermann H. P. and Buenker R. J.
- 103402 Site preferences and lattice vibrations of $\text{Nd}_6\text{Fe}_{13-x}\text{T}_x\text{Si}$ ($T = \text{Co, Ni}$)**
Huang Tian-Shun, Cheng Hai-Xia, Wang Xiao-Xu, Zhang Zhen-Feng, An Zhi-Wei and Zhang Guo-Hua
- 103403 Single ionization of helium atoms by energetic fully stripped carbon ions**
Ebrahim Ghanbari-Adivi and Sadjad Eskandari
- 103601 Modeling the interaction of nitrate anions with ozone and atmospheric moisture**
A. Y. Galashev

ELECTROMAGNETISM, OPTICS, ACOUSTICS, HEAT TRANSFER, CLASSICAL MECHANICS, AND FLUID DYNAMICS

- 104101 Reciprocity principle-based model for shielding effectiveness prediction of a rectangular cavity with a covered aperture**
Jiao Chong-Qing and Li Yue-Yue
- 104102 Design and development of high linearity millimeter wave traveling-wave tube for satellite communications**
He Jun, Huang Ming-Guang, Li Xian-Xia, Li Hai-Qiang, Zhao Lei, Zhao Jian-Dong, Li Yue and Zhao Shi-Lei
- 104103 Exploring electromagnetic response of tellurium dielectric resonator metamaterial at the infrared wavelengths**
Song Jia-Kun, Song Yu-Zhi, Li Kang-Wen, Zhang Zu-Yin, Xu Yun, Wei Xin and Song Guo-Feng
- 104104 Tunable wideband absorber based on resistively loaded lossy high-impedance surface**
Dang Ke-Zheng, Shi Jia-Ming, Wang Jia-Chun, Lin Zhi-Dan and Wang Qi-Chao
- 104201 Absorption enhancement in thin film a-Si solar cells with double-sided SiO_2 particle layers**
Chen Le, Wang Qing-Kang, Shen Xiang-Qian, Chen Wen, Huang Kun and Liu Dai-Ming
- 104202 Superscattering-enhanced narrow band forward scattering antenna**
Hu De-Jiao, Zhang Zhi-You and Du Jing-Lei
- 104203 Ghost imaging with broad distance**
Duan De-Yang, Zhang Lu, Du Shao-Jiang and Xia Yun-Jie

(Continued on the Bookbinding Inside Back Cover)

- 104204 An iterative virtual projection method to improve the reconstruction performance for ill-posed emission tomographic problems**
Liu Hua-Wei, Zheng Shu and Zhou Huai-Chun
- 104205 Field-free orientation of diatomic molecule via the linearly polarized resonant pulses**
Li Su-Yu, Guo Fu-Ming, Wang Jun, Yang Yu-Jun and Jin Ming-Xing
- 104206 Photon pair source via two coupling single quantum emitters**
Peng Yong-Gang and Zheng Yu-Jun
- 104207 Movement of a millimeter-sized oil drop pushed by optical force**
Zhang Li and She Wei-Long
- 104208 Entanglements in a coupled cavity–array with one oscillating end-mirror**
Wu Qin, Xiao Yin and Zhang Zhi-Ming
- 104209 Plasmonic emission and plasma lattice structures induced by pulsed laser in Purcell cavity on silicon**
Huang Wei-Qi, Huang Zhong-Mei, Miao Xin-Jian, Liu Shi-Rong and Qin Chao-Jian
- 104210 Analysis of gain distribution in cladding-pumped thulium-doped fiber laser and optical feedback inhibition problem in fiber-bulk laser system**
Ji En-Cai, Liu Qiang, Hu Zhen-Yue and Gong Ma-Li
- 104211 Arbitrary frequency stabilization of a diode laser based on visual Labview PID VI and sound card output**
Feng Guo-Sheng, Wu Ji-Zhou, Wang Xiao-Feng, Zheng Ning-Xuan, Li Yu-Qing, Ma Jie, Xiao Lian-Tuan and Jia Suo-Tang
- 104212 Broadband and high-speed swept external-cavity laser using a quantum-dot superluminescent diode as gain device**
Hu Fa-Jie, Jin Peng, Wu Yan-Hua, Wang Fei-Fei, Wei Heng and Wang Zhan-Guo
- 104213 An optical fiber spool for laser stabilization with reduced acceleration sensitivity to $10^{-12}/g$**
Hu Yong-Qi, Dong Jing, Huang Jun-Chao, Li Tang and Liu Liang
- 104214 V–L decomposition of a novel full-waveform lidar system based on virtual instrument technique**
Xu Fan and Wang Yuan-Qing
- 104215 Confinement-induced nanocrystal alignment of conjugated polymer by the soft-stamped nanoimprint lithography**
Li Xiao-Hui, Yu Ji-Cheng, Lu Nai-Yan, Zhang Wei-Dong, Weng Yu-Yan and Gu Zhen
- 104216 Analysis of the spatial filter of a dielectric multilayer film reflective cutoff filter-combination device**
Zhang Ying, Qi Hong-Ji, Yi Kui, Wang Yan-Zhi, Sui Zhan and Shao Jian-Da
- 104301 Quantitative calculation of reaction performance in sonochemical reactor by bubble dynamics**
Xu Zheng, Yasuda Keiji and Liu Xiao-Jun
- 104302 Wavefront modulation of water surface wave by a metasurface**
Sun Hai-Tao, Cheng Ying, Wang Jing-Shi and Liu Xiao-Jun

104303 Temperature imaging with speed of ultrasonic transmission tomography for medical treatment control: A physical model-based method

Chu Zhe-Qi, Yuan Jie, Stephen Z. Pinter, Oliver D. Kripfgans, Wang Xue-Ding, Paul L. Carson and Liu Xiao-Jun

104501 Nonlinear parametrically excited vibration and active control of gear pair system with time-varying characteristic

Liu Shuang, Wang Jin-Jin, Liu Jin-Jie and Li Ya-Qian

104502 Skew-gradient representation of generalized Birkhoffian system

Mei Feng-Xiang and Wu Hui-Bin

104701 Effects of the computational domain on the secondary flow in turbulent plane Couette flow

Gai Jie, Xia Zhen-Hua and Cai Qing-Dong

104702 Ferrofluid nucleus phase transitions in an external uniform magnetic field

B. M. Tanygin, S. I. Shulyma, V. F. Kovalenko and M. V. Petrychuk

PHYSICS OF GASES, PLASMAS, AND ELECTRIC DISCHARGES

105101 Dynamic mechanical analysis of single walled carbon nanotubes/polymethyl methacrylate nanocomposite films

Ali Badawi and N. Al-Hosiny

105102 Effect of microwave frequency on plasma formation in air breakdown at atmospheric pressure

Zhao Peng-Cheng, Guo Li-Xin and Li Hui-Min

105201 Investigation of high sensitivity radio-frequency readout circuit based on AlGaIn/GaN high electron mobility transistor

Zhang Xiao-Yu, Tan Ren-Bing, Sun Jian-Dong, Li Xin-Xing, Zhou Yu, Lü Li and Qin Hua

CONDENSED MATTER: STRUCTURAL, MECHANICAL, AND THERMAL PROPERTIES

106101 Complementary method to locate atomic coordinates by combined searching method of structure-sensitive indexes based on bond valence method

Song Zhen, Liu Xiao-Lang, He Li-Zhu, Xia Zhi-Guo and Liu Quan-Lin

106102 Influences of surface and flexoelectric polarization on the effective anchoring energy in nematic liquid crystal

Guan Rong-Hua, Ye Wen-Jiang and Xing Hong-Yu

106103 Determination of electrostatic parameters of a coumarin derivative compound $C_{17}H_{13}NO_3$ by x-ray and density functional theory

Youcef Megrouss, Nadia Benhalima, Rawia Bahoussi, Nouredine Boukabcha, Abdelkader Chouaih and Fodil Hamzaoui

106104 New crystal structure and physical properties of TcB from first-principles calculations

Zhang Gang-Tai, Bai Ting-Ting, Yan Hai-Yan and Zhao Ya-Ru

106105 Influences of neutral oxygen vacancies and E'_1 centers on α -quartz

Li Hui-Ran, Cheng Xin-Lu, Zhang Hong and Zhao Feng

106106 Analysis of functional failure mode of commercial deep sub-micron SRAM induced by total dose irradiation

Zheng Qi-Wen, Cui Jiang-Wei, Zhou Hang, Yu De-Zhao, Yu Xue-Feng, Lu Wu, Guo Qi and Ren Di-Yuan

106601 Analysis of recoverable and permanent components of threshold voltage shift in NBT stressed p-channel power VDMOSFET

Danijel Danković, Ninoslav Stojadinović, Zoran Prijić, Ivica Manić, Vojkan Davidović, Aneta Prijić, Snežana Djorić-Veljković and Snežana Golubović

106801 Mechanical strains in pecvd SiN_x:H films for nanophotonic application

O. Semenova, A. Kozelskaya, Li Zhi-Yong, and Yu Yu-De

CONDENSED MATTER: ELECTRONIC STRUCTURE, ELECTRICAL, MAGNETIC, AND OPTICAL PROPERTIES

107101 Structural, elastic, and electronic properties of sodium atoms encapsulated type-I silicon-clathrate compound under high pressure

Zhang Wei, Chen Qing-Yun, Zeng Zhao-Yi and Cai Ling-Cang

107102 Nano LaAlO₃ buffer layer-assisted tunneling current in manganite p-n heterojunction

Ma Jun-Jie, Wang Deng-Jing, Huang Hai-Lin, Wang Ru-Wu and Li Yun-Bao

107301 Influences of Pr and Ta doping concentration on the characteristic features of FTO thin film deposited by spray pyrolysis

Güven Turgut, Adem Koçyiğit and Erdal Sönmez

107302 High response Schottky ultraviolet photodetector formed by PEDOT:PSS transparent electrode contacts to Mg_{0.1}Zn_{0.9}O

Hu Zuo-Fu, Wu Huai-Hao, Lv Yan-Wu and Zhang Xi-Qing

107303 Effect of the annealing temperature on the long-term thermal stability of Pt/Si/Ta/Ti/4H-SiC contacts

Cheng Yue, Zhao Gao-Jie, Liu Yi-Hong, Sun Yu-Jun, Wang Tao and Chen Zhi-Zhan

107304 Rectification and electroluminescence of nanostructured GaN/Si heterojunction based on silicon nanoporous pillar array

Wang Xiao-Bo, Li Yong, Yan Ling-Ling and Li Xin-Jian

107305 A C-band 55% PAE high gain two-stage power amplifier based on AlGaIn/GaN HEMT

Zheng Jia-Xin, Ma Xiao-Hua, Lu Yang, Zhao Bo-Chao, Zhang Hong-He, Zhang Meng, Cao Meng-Yi and Hao Yue

107306 Fermi level pinning effects at gate-dielectric interfaces influenced by interface state densities

Hong Wen-Ting, Han Wei-Hua, Lyu Qi-Feng, Wang Hao and Yang Fu-Hua

107307 Lateral resistance reduction induced by light-controlled leak current in silicon-based Schottky junction

Wang Shuan-Hu, Zhang Xu, Zou Lv-Kuan, Zhao Jing, Wang Wen-Xin and Sun Ji-Rong

107501 Magnetic hysteresis, compensation behaviors, and phase diagrams of bilayer honeycomb lattices

Ersin Kantar

- 107502 Exact solution of Heisenberg model with site-dependent exchange couplings and Dzyloshinsky–Moriya interaction**
Yang Li-Jun, Cao Jun-Peng and Yang Wen-Li
- 107503 Effects of oxidation of DyH₃ in Nd–Fe–B sintered magnets**
Yan Gao-Lin and Fang Zhi-Hao
- 107504 Effects of R-site compositions on the meta-magnetic behavior of Tb_{1-x}Pr_x(Fe_{0.4}Co_{0.6})_{1.88}C_{0.05} (x = 0, 0.8, and 1)**
Huang Jun-Wei, Xia Zheng-Cai, Cheng Gang, Shi Li-Ran, Jin Zhao, Shang Cui and Wei Meng
- 107505 Magnetic–optical bifunctional CoPt₃/Co multilayered nanowire arrays**
Su Yi-Kun, Yan Zhi-Long, Wu Xi-Ming, Liu Huan, Ren Xiao and Yang Hai-Tao
- 107506 Lumped-equivalent circuit model for multi-stage cascaded magnetoelectric dual-tunable bandpass filter**
Zhang Qiu-Shi, Zhu Feng-Jie and Zhou Hao-Miao
- 107701 The interface density dependence of the electrical properties of 0.9Pb(Sc_{0.5}Ta_{0.5})O₃–0.1PbTiO₃/0.55Pb(Sc_{0.5}Ta_{0.5})O₃–0.45PbTiO₃ multilayer thin films**
Li Xue-Dong, Liu Hong, Wu Jia-Gang, Liu Gang, Xiao Ding-Quan and Zhu Jian-Guo
- 107702 Nanoscale domain switching mechanism of Bi_{3.15}Eu_{0.85}Ti₃O₁₂ thin film under the different mechanical forces**
Zhu Zhe, Chen Yu-Bo and Zheng Xue-Jun
- 107703 Effects of surface adsorbed oxygen, applied voltage, and temperature on UV photoresponse of ZnO nanorods**
Zong Xian-Li and Zhu Rong
- 107704 C–H complex defects and their influence in ZnO single crystal**
Xie Hui, Zhao You-Wen, Liu Tong, Dong Zhi-Yuan, Yang Jun and Liu Jing-Ming
- 107705 Temperature dependences of ferroelectricity and resistive switching behavior of epitaxial BiFeO₃ thin films**
Lu Zeng-Xing, Song Xiao, Zhao Li-Na, Li Zhong-Wen, Lin Yuan-Bin, Zeng Min, Zhang Zhang, Lu Xu-Bing, Wu Su-Juan, Gao Xing-Sen, Yan Zhi-Bo and Liu Jun-Ming
- 107801 Multifunctional disk device for optical switch and temperature sensor**
Bian Zhen-Yu, Liang Rui-Sheng, Zhang Yu-Jing, Yi Li-Xuan, Lai Gen and Zhao Rui-Tong
- 107802 Single-layer dual-band terahertz filter with weak coupling between two neighboring cross slots**
Qi Li-Mei, Li Chao, Fang Guang-You and Li Shi-Chao
- 107803 Simulation of positron backscattering and implantation profiles using Geant4 code**
Huang Shi-Juan, Pan Zi-Wen, Liu Jian-Dang, Han Rong-Dian and Ye Bang-Jiao
- 107804 Exploring positron characteristics utilizing two new positron–electron correlation schemes based on multiple electronic structure calculation methods**
Zhang Wen-Shuai, Gu Bing-Chuan, Han Xiao-Xi, Liu Jian-Dang and Ye Bang-Jiao

(Continued on the Bookbinding Inside Back Cover)

INTERDISCIPLINARY PHYSICS AND RELATED AREAS OF SCIENCE AND TECHNOLOGY

- 108101 Temperature-dependent photoluminescence spectra of GaN epitaxial layer grown on Si (111) substrate**
Zhao Dan-Mei, Zhao De-Gang, Jiang De-Sheng, Liu Zong-Shun, Zhu Jian-Jun, Chen Ping, Liu Wei, Li Xiang and Shi Ming
- 108102 Influences of hydrogen dilution on microstructure and optical absorption characteristics of nc-SiO_x:H film**
Zhao Wei, Du Lin-Yuan, Jiang Zhao-Yi, Yin Chen-Chen, Yu Wei and Fu Guang-Sheng
- 108201 Ion and water transport in charge-modified graphene nanopores**
Qiu Ying-Hua, Li Kun, Chen Wei-Yu, Si Wei, Tan Qi-Yan and Chen Yun-Fei
- 108202 Surface morphology and electrochemical characterization of electrodeposited Ni–Mo nanocomposites as cathodes for hydrogen evolution**
Elhachmi Guettaf Temam, Hachemi Ben Temam and Said Benramache
- 108203 Closed-form solution of mid-potential between two parallel charged plates with more extensive application**
Shang Xiang-Yu, Yang Chen and Zhou Guo-Qing
- 108401 Dual-band LTCC antenna based on 0.95Zn₂SiO₄-0.05CaTiO₃ ceramics for GPS/UMTS applications**
Dou Gang, Li Yu-Xia and Guo Mei
- 108402 Charge and spin-dependent thermal efficiency of polythiophene molecular junction in presence of dephasing**
Z. Golsanamlou, M. Bagheri Tagani and H. Rahimpour Soleimani
- 108501 Simulation study of the losses and influences of geminate and bimolecular recombination on the performances of bulk heterojunction organic solar cells**
Zhu Jian-Zhuo, Qi Ling-Hui, Du Hui-Jing and Chai Ying-Chun
- 108502 An improved GGNMOS triggered SCR for high holding voltage ESD protection applications**
Zhang Shuai, Dong Shu-Rong, Wu Xiao-Jing, Zeng Jie, Zhong Lei and Wu Jian
- 108503 A novel diode string triggered gated-PiN junction device for electrostatic discharge protection in 65-nm CMOS technology**
Zhang Li-Zhong, Wang Yuan, Lu Guang-Yi, Cao Jian and Zhang Xing
- 108504 Electrical properties of zinc-oxide-based thin-film transistors using strontium-oxide-doped semiconductors**
Wu Shao-Hang, Zhang Nan, Hu Yong-Sheng, Chen Hong, Jiang Da-Peng and Liu Xing-Yuan
- 108505 A threshold voltage model of short-channel fully-depleted recessed-source/drain (Re-S/D) SOI MOS-FETs with high-*k* dielectric**
Gopi Krishna Saramakala, Sarvesh Dubey and Pramod Kumar Tiwari
- 108506 Fabrication and characterization of novel high-speed InGaAs/InP uni-traveling-carrier photodetector for high responsivity**
Chen Qing-Tao, Huang Yong-Qing, Fei Jia-Rui, Duan Xiao-Feng, Liu Kai, Liu Feng, Kang Chao, Wang Jun-Chu, Fang Wen-Jing and Ren Xiao-Min

- 108701 Ultrafast structural dynamics studied by kilohertz time-resolved x-ray diffraction**
Guo Xin, Jiang Zhou-Ya, Chen Long, Chen Li-Ming, Xin Jian-Guo, Peter M. Rentzepis and Chen Jie
- 108702 Investigation of noise properties in grating-based x-ray phase tomography with reverse projection method**
Bao Yuan, Wang Yan, Gao Kun, Wang Zhi-Li, Zhu Pei-Ping and Wu Zi-Yu
- 108703 Flexible-reduced field of view magnetic resonance imaging based on single-shot spatiotemporally encoded technique**
Li Jing, Cai Cong-Bo, Chen Lin, Chen Ying, Qu Xiao-Bo and Cai Shu-Hui
- 108801 Analysis of the interdigitated back contact solar cells: The n-type substrate lifetime and wafer thickness**
Zhang Wei, Chen Chen, Jia Rui, Sun Yun, Xing Zhao, Jin Zhi, Liu Xin-Yu and Liu Xiao-Wen
- 108802 GaInP/GaAs tandem solar cells with highly Te- and Mg-doped GaAs tunnel junctions grown by MBE**
Zheng Xin-He, Liu San-Jie, Xia Yu, Gan Xing-Yuan, Wang Hai-Xiao, Wang Nai-Ming and Yang Hui
- 108901 Improved routing strategy based on gravitational field theory**
Song Hai-Quan and Guo Jin

GEOPHYSICS, ASTRONOMY, AND ASTROPHYSICS

- 109201 Spatiotemporal distribution characteristics and attribution of extreme regional low temperature event**
Feng Tai-Chen, Zhang Ke-Quan, Su Hai-Jing, Wang Xiao-Juan, Gong Zhi-Qiang and Zhang Wen-Yu

JUST FOR AUTHORS
— CHINESE PHYSICS B